International Journal on Smart Material and Mechatronics
IJSMM Vol. 12 No.2 2025 DOI. 10.20342/IJSMM.10.1. 391
p-ISSN: 2356-5314
e-ISSN: 2460-075X

CFD Simulation of an Ocean Current Turbine Energy Converter with Dynamic Electric Load at Kepa Strait, Indonesia

Rizki Pratama Putra
Automation Engineering, Dept Engineering
Universitas Negeri Jakarta, Indonesia
rizki.pratama@unj.ac.id

***Abstract*—The interaction of fluids and turbines in ocean current energy converter systems is a crucial step to be studied in realizing ocean current energy converters. In this study, a marine current turbine system was simulated in conditions connected to a loaded generator with a constant ocean current inlet, to investigate the dynamic characteristics of the turbine under that condition. The simulation was carried out using the Computational Fluid Dynamic (CFD) technique in Ansys software to observe the characteristics of no-load and loaded turbines. The results show that loading the turbine-generator system results in a decrease in the average value of the turbine angular velocity, together with a reduction in the angular velocity spikes that were previously present in the unloaded condition. In the fluid velocity contours, it can be seen that under loaded conditions the turbulence around the blade becomes higher because the turbine rotation slows down slightly, which in theory can reduce the energy conversion efficiency of the turbine-generator system.**

***Index Terms*—Computational Fluid Dynamic, Ocean Current Energy Converter, Airfoil, Vertical Shaft Turbine**

I. Introduction

Strong ocean currents in the waters of East Nusa Tenggara, based on research conducted by [1], show relatively large potential for building ocean current power plants. Indonesia itself is an archipelagic country where sea currents are quite strong, especially in the straits between islands. However, just like other renewable energy sources, ocean currents are not stable or intermittent, so if used directly without a control system they can damage the existing consumer electricity system.

In the process of building ocean current power plants, studies related to simulating plant performance against changing loads need to be carried out before procuring physical equipment. Several studies have simulated the performance of ocean current power plants with various methods that provide accurate results, including research on the influence of surface waves on the hydrodynamic performance of horizontal axis turbines [2]. That study simulated fluid interactions using CFD to analyse the performance of horizontal axis turbines placed at varying depths, and the results show torque oscillations that vary with turbine depth. The accuracy of CFD in simulating turbine-fluid interactions has also been investigated by Guo [3], where the BEM-CFD method was used to simulate horizontal turbine and fluid interactions; the study found that the simulation results had good accuracy at optimal conditions (TSR = 5–7), and poor results outside the optimal conditions. A review of the accuracy of computational fluid techniques for vertical turbines has been discussed by Masoud [4], presenting guidelines and recommendations for conducting accurate CFD simulations, including a comparison of CFD computing techniques.

Meanwhile, in its application, ocean current power plants will always be in changing load conditions. Related research on the use of CFD in ocean wave power plant applications includes that conducted by Cui [5], where fluid computational techniques were used to optimize the geometry of axial turbines for ocean wave energy converters. The performance evaluation of ocean wave power plants was studied by Zhang [6] using analytical techniques. Similar work was carried out by Sergiienko [7] on a three-tether axisymmetric wave energy converter and by Liang [8] on OWC performance with mechanical motion rectifiers. Both studies did not involve dynamic fluid computation to investigate the characteristics of the OWC, since systems consisting of turbines, generators, and PTO are more efficiently simulated without the high computational resources required by CFD.

The studies mentioned above mostly examine the effects of loading on plants using analytical methods, and only a small part using numerical methods. For the interaction of ocean currents and turbine converters, the more complicated the turbine design, the more difficult it becomes to find the output power characteristics of the turbine using analytical techniques. To solve the problem of fluid-object interaction, fluid computational techniques are therefore often used.

In this study, a sea current power plant is simulated under loaded conditions to observe the characteristics of the output power and speed produced. The simulation is carried out using CFD techniques in Ansys software.

II. Methods

A. System Schematic

The schematic drawing of the simulated system is shown in Fig. 1. Based on the schematic, input data is taken from statistical data of sea currents in the Kepa Strait over 15 days, and the average current value is used as the simulation input. In the simulation, an electric torque is included as a preload.

Fig. 1. System schematic of the ocean current turbine energy converter.

B. Electric Load

The Fluent solver can only accept mechanical loads, so electrical loads must first be converted to an equivalent mechanical load, applied as a preload torque. For a permanent

p-ISSN: 2356-5314
e-ISSN: 2460-075X

magnet synchronous machine with Ld = Lq, the electric torque can be found using the following equation:

$$\tau_e = (3/2)\, k_t\, i_l \qquad (1)$$

where τe is the electric torque (N.m), kt is the torque constant, and il is the line current. The simulated load used in this study can be seen in Table I.

TABLE 1. SIMULATED ELECTRIC LOAD

No	Electric Load (kW)	Electric Torque (N.m)
1	0	0
2	1 kW	4.32

C. Turbine Geometry

The turbine used is a Vertical Axis (Savonius) type with a blade cross-sectional length of 300 mm, as shown in Fig. 2.

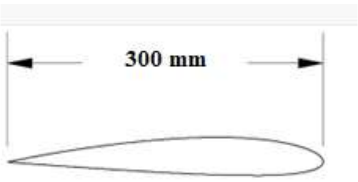

Fig. 2. Cross-sectional dimensions of the turbine blade.

The airfoil used refers to the NACA airfoil standard, which has become a general standard where the shape has been optimized so that the resulting lift is optimal and inefficiency due to turbulence can be minimized. This type of airfoil has been widely used in vertical turbines, as in [9], which compares turbines with 2 blades and 3 blades based on CFD simulation results. The details of the airfoil used are shown in Table II.

TABLE 2. AIRFOIL GEOMETRY

No	Parameter	Value
1	Max Chamber	2%
2	Max Chamber position	40%
3	Thickness	12%
4	Number of points	200
5	Trailing edge	Closed

The turbine parameters used are shown in detail in Table III.

TABLE 3. TURBINE SPECIFICATION

No	Parameter	Value
1	Material	PVC (blade), Aluminium 6061 (rotor shaft and blade holder)
2	Total mass	86.863 kg
3	Inertia	146.417 kg.m²
4	Height	3.6 m
5	Diameter	3.6 m
6	Blade wall thickness	2.5 mm
7	Shaft diameter	200 mm
8	Shaft wall thickness	3 mm

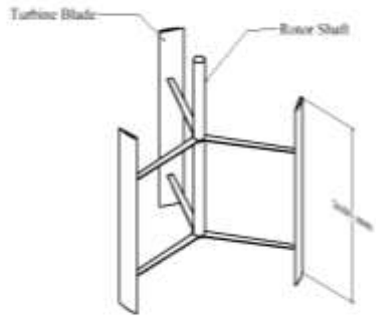

Fig. 3. Turbine CAD model.

The type of turbine used in the simulation is the Savonius turbine, which is often used in low-speed wind turbine applications and has also been frequently used in simulations such as those conducted by Afif [10], Didane [11], and Franchina [12], where CFD is used to evaluate and optimize turbine designs. In this study, the Savonius turbine used consists of 3 blades, each with a length of 3.6 m and a turbine diameter of 3.6 m. The thickness of the blades is obtained based on the geometry of the NACA airfoil. In research conducted by Ostos [13], it is known that the thickness of the horizontal turbine blade affects the power that can be generated by the turbine; however, in this study, the scope was limited to the effect of loading on vertical turbines with blades following the NACA airfoil standard shape. The turbine blades are fastened by spokes made of aluminum with a thickness of 10 mm. The turbine shaft is made of aluminum pipe with a thickness of 3 mm and a diameter of 200 mm, designed with such a shape and size to withstand the mechanical force of the seawater push while remaining lightweight.

D. Simulation Zone

In the simulation process using Ansys, the simulation geometry describes the fluid flow zone, the turbine rotation zone, and the turbine zone itself, as shown in Fig. 4.

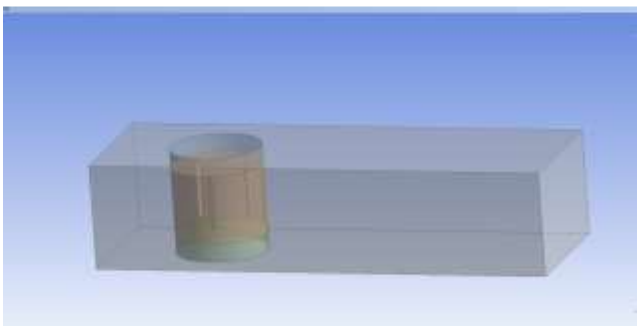

Fig. 4. Simulation zone in Ansys software.

E. Meshing

The meshing process is carried out with attention to the specifications of the computer used. The meshing parameters used are shown in Table IV.

TABLE 4. MESHING PARAMETERS

No	Parameter	Zone	Value
1	Sizing	Turbine	0.03 m

p-ISSN: 2356-5314
e-ISSN: 2460-075X

No	Parameter	Zone	Value
2		Upper rotation zone	0.15 m
3		Center rotation zone	0.15 m
4		Bottom rotation zone	0.15 m
5		Fluid flow zone	0.6 m
6	Method	Upper/lower rotation zones, fluid flow	Multizone-hexa/prism

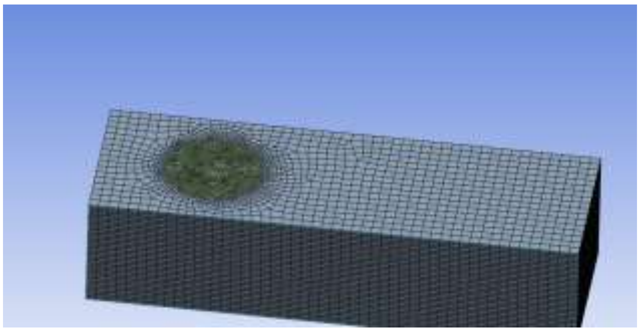

Fig. 5. Meshing result.

F. Setup Parameter

The Ansys Fluent setup section provides the input data, simulation method settings, and output data reading. Detailed simulation settings are given in Table V.

TABLE 5. PARAMETERS SETUP

No	Parameter	Value
1	Time simulation	Transient, 20 s
2	Viscous model	k-epsilon
3	Material fluid density	1025 kg/m³
4	Material fluid viscosity	0.000928 kg/ms
5	Boundary condition (inlet)	1.324*(1-exp(-Time/0.5)) m/s
6	Dynamic mesh (turbine mass)	86.863 kg
7	Dynamic mesh (turbine inertia)	146.417 kg.m²
8	Number of time step	400
9	Time step size	0.05 s
10	Max iteration/time step	50

III. RESULTS AND DISCUSSION

A. Output Power and Dynamic Speed Response of Turbines

The simulation results using Ansys Fluent, based on the input data described above, are presented below. From Fig. 6, the dynamic power of the turbine looks more fluctuating in the no-load condition compared to the loaded condition. Power changes occur periodically under loaded conditions, while in the no-load condition, spikes in power change often appear. The electric load here acts like a damper for these fluctuations. Based on rotational kinematics, angular acceleration is affected by the torques acting on the solid body, so the increase in damping torque coming from the electrical load reduces the angular acceleration of the turbine system.

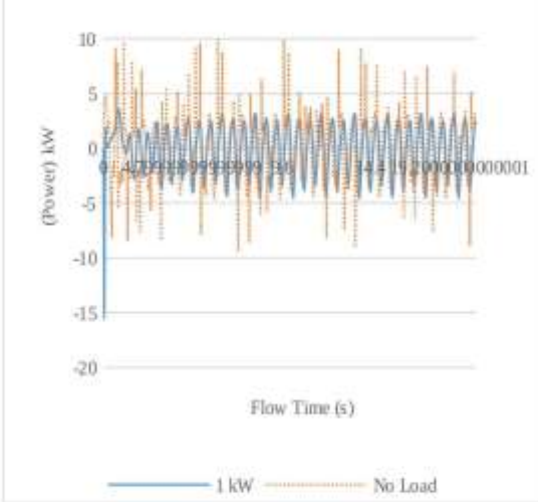

Fig. 6. Dynamic power response of the turbine.

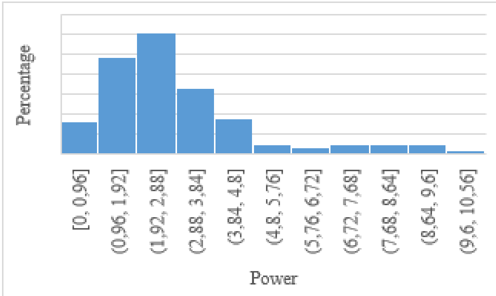

Fig. 7. Power histogram (no load).

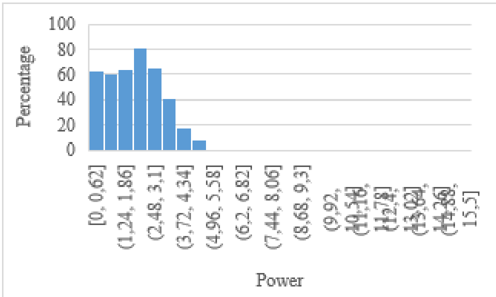

Fig. 8. Power histogram (load 1 kW).

TABLE 6. AVERAGE POWER OF THE TURBINE

No Load	1 kW
2.91331 kW	1.96845 kW

From the power histogram and the average power value, it can also be seen that the power produced by the fluid decreases with the addition of electrical load. This happens because of the decrease in the turbine's angular velocity, which can be seen in the following results. In the no-load condition, the torque acting on the turbine is only the torque derived from the momentum of the fluid interacting with the turbine blade, so the power generated fluctuates depending on the angle of interaction between the fluid and the blade. Under loaded conditions, torque fluctuations from the fluid are dampened by the negative torque derived from the electrical load, so that the power changes become more regular.

p-ISSN: 2356-5314
e-ISSN: 2460-075X

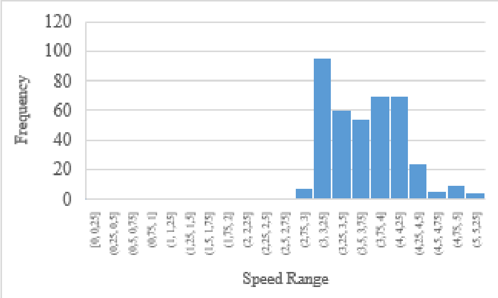

Fig. 9. Turbine dynamic speed histogram (no load).

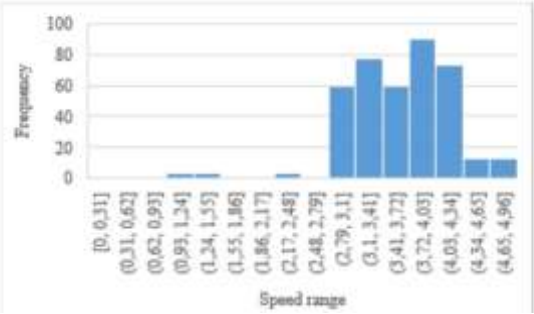

Fig. 10. Turbine dynamic speed histogram (loaded).

B. Angular Velocity

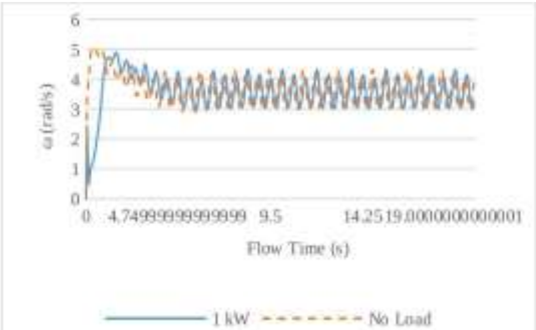

Fig. 11. Angular velocity of the turbine.

TABLE 7. AVERAGE ANGULAR SPEED OF THE TURBINE

No Load	Load 1 kW
3.67025 rad/s	3.5958 rad/s

From Fig. 11 and Table VII it can be seen that, in general, the output power — or in this case the capable power produced by the turbine — decreases with the increase in electrical load, and in the no-load condition the capable power of the turbine reaches its maximum value. The same trend can be seen in the rotational speed of the turbine, which decreases with increasing electrical load.

This occurs due to energy conservation, where energy only changes form: previously in the form of turbine kinetic energy (turbine rotation), then after the electrical load is connected, the rotational or kinetic energy of the turbine is reduced. At that point, the total energy of the system is the kinetic energy still stored in the turbine plus the electrical energy channeled to the load. The impact of the decreasing rotational speed of the turbine is a decrease in the frequency of the electric voltage produced (if a direct-drive model is used).

C. Contours of Fluid Velocity around the Turbine

Fig. 12 and Fig. 13 show the contours of the fluid velocity around the turbine in the no-load and loaded simulations, respectively.

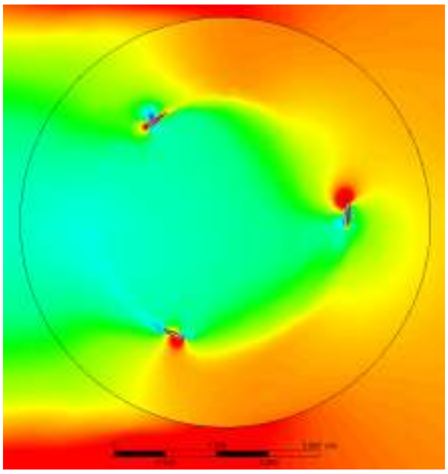

Fig. 12. Contours of fluid velocity (no-load turbine condition).

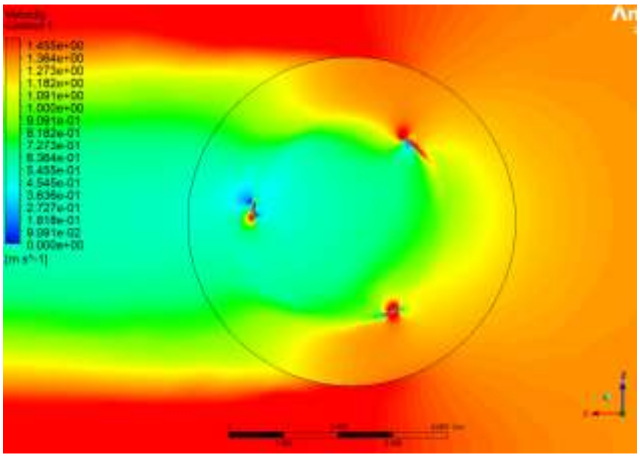

Fig. 13. Contours of fluid velocity (load condition).

It can be seen that the turbulence of fluid flow around the turbine burdened by electrical power is greater than that of the turbine without load. This can be observed from the velocity gradient at the tip of the larger blade. Turbulence of fluid flow around solid objects always occurs, and its magnitude depends on the geometry of the object and the angle of interaction.

In the simulation, the airfoil has been designed to maximize energy conversion and minimize the effects of fluid flow turbulence that can reduce energy conversion efficiency. The effect of turbulence depends on the angle of interaction between the airfoil and the fluid. The slowing of turbine rotation causes the interaction time between the airfoil and the fluid to be longer, so that the effect of fluid reflection and fluid flow turbulence becomes more intense. This, in turn, reduces the energy conversion efficiency of the turbine-fluid system.

IV. CONCLUSION

1. The increase in electrical load causes the turbine rotation to become heavier. This is due to the load torque opposing the torque derived from the fluid-turbine interaction.

p-ISSN: 2356-5314
e-ISSN: 2460-075X

2. The entry of electric torque into the system makes the angular velocity spikes more stable, while the angular velocity frequency in steady-state conditions tends not to change.

3. From the simulation results it is also seen that the total power in the system increases under load conditions compared to unloaded conditions for the 1 kW load tested; further investigation of variable loads is needed.

4. From the contour map of the fluid velocity around the turbine blade, it can be observed that the turbulence of the fluid flow becomes higher when the turbine experiences the opposing torque from the electrical load. This is due to the longer angular interaction time of the turbine fluid-blade, which reduces the energy conversion efficiency of the turbine system.

REFERENCES

[1] Orhan, K., & Mayerle, R. (2017). Assessment of the tidal stream power potential and impacts of tidal current turbines in the Strait of Larantuka, Indonesia. Energy Procedia, 125, 230–239.

[2] Tian, W., Song, B., VanZwieten, J. H., & Pyakurel, P. (2020). Influence of surface waves on the hydrodynamic performance of a horizontal axis ocean current turbine. Renewable Energy, 158, 37–48.

[3] Guo, Q., Zhou, L., & Wang, Z. (2015). Comparison of BEM-CFD and full rotor geometry simulations for the performance and flow field of a marine current turbine. Renewable Energy, 75, 640–648.

[4] Ghasemian, M., Najafian Ashrafi, Z., & Sedaghat, A. (2017). A review on computational fluid dynamic simulation techniques for Darrieus vertical axis wind turbines. Energy Conversion and Management, 149, 87–100.

[5] Cui, Y., et al. (2019). Review of CFD studies on axial-flow self-rectifying turbines for OWC wave energy conversion. Ocean Engineering, 175, 80–102.

[6] Zhang, Y., et al. (2021). Ocean wave energy converters: Technical principle, device realization, and performance evaluation. Renewable and Sustainable Energy Reviews, 141, 110764.

[7] Sergiienko, N. Y., et al. (2018). Feasibility study of the three-tether axisymmetric wave energy converter. Ocean Engineering, 150, 221–233.

[8] Liang, C., Ai, J., & Zuo, L. (2017). Design, fabrication, simulation, and testing of an ocean wave energy converter with mechanical motion rectifier. Ocean Engineering, 136, 190–200.

[9] Subramanian, A., et al. (2017). Effect of airfoil and solidity on the performance of small scale vertical axis wind turbine using three dimensional CFD model. Energy, 133, 179–190.

[10] Afif, A. A., Wulandari, P., & Syahriar, A. (2020). CFD analysis of vertical axis wind turbine using ansys fluent. Journal of Physics: Conference Series, 1517(1).

[11] Didane, D. H., et al. (2022). Performance investigation of vertical axis wind turbine with Savonius rotor using computational fluid dynamics (CFD). CFD Letters, 14(8), 116–124.

[12] Franchina, N., et al. (2019). Three-dimensional CFD simulation and experimental assessment of the performance of an H-shape vertical-axis wind turbine at design and off-design conditions. International Journal of Turbomachinery, Propulsion, and Power, 4(3), 30.

[13] Ostos, I., et al. (2019). A modified novel blade configuration proposal for a more efficient VAWT using CFD tools. Energy Conversion and Management, 180, 733–746.